PROCEEDINGS OF SPIE

SPIEDigitalLibrary.org/conference-proceedings-of-spie

High-speed data acquisition and computing for real-time active control of civil structures subject to seismic base excitation

Peckens, Courtney

Courtney A. Peckens, "High-speed data acquisition and computing for real-time active control of civil structures subject to seismic base excitation," Proc. SPIE 12046, Sensors and Smart Structures Technologies for Civil, Mechanical, and Aerospace Systems 2022, 1204602 (18 April 2022); doi: 10.1117/12.2612570



Event: SPIE Smart Structures + Nondestructive Evaluation, 2022, Long Beach, California, United States

High-speed data acquisition and computing for real-time active control of civil structures subject to seismic base excitation

Courtney A. Peckens*a aDept. of Engineering, Hope College, 27 Graves Place, Holland, MI, USA 49422-9000

ABSTRACT

Active structural control of civil infrastructure in response to large external loads, such as earthquake or wind, requires the rapid integration of information between sensing nodes, computational nodes, and actuating nodes. Because of this, it is still not widely employed due to several key issues, such as latency in the system and challenges with information exchange. In this study, the *Martlet*, a high-speed data acquisition and computing node that was designed based on a Texas Instruments Piccolo microcontroller and capable of peer-to-peer wireless communication, is used for all three steps in the active control process. For rapid sensing, the *Martlet* is equipped with an interface board that interfaces with a displacement transducer and has an on-board differentiating circuit to derive velocity. The sensing *Martlet* transmits its data (i.e., displacement and velocity) to the actuating *Martlet*. The actuating *Martlet* calculates the necessary control force using an optimal control law, the full-state linear quadratic regulator. The resulting control force is then conveyed to the actuator via a controller interface board. This complete process is experimentally validated on a partial-scale, four-story shear structure and it is demonstrated that due to the fast processing speeds of the *Martlet*, real-time control of the structure can be achieved.

Keywords: Structural control, wireless sensor networks, active control

1. INTRODUCTION

Control of civil infrastructure (e.g., buildings and bridges) has been explored over the last several decades as one method for mitigating undesired response and destruction when subject to large external loads, such as seismic events or high winds¹. Active control techniques offer real-time adaptability, as well as specific selectivity of control objectives, which other control methods often lack. This method, however, requires effective collaboration between sensors that measure the response of the structure (e.g., displacement, velocity), computational nodes that determine the appropriate reaction to the response of the structure, and actuators which supply the desired response. For numerous years, communication between these entities was conducted using cables^{2,3}, which were cumbersome to install and resulted in reduced communication capabilities, but in recent years, wireless telemetry has replaced the cables as a viable mode of communication.

With the addition of wireless telemetry nodes are equipped to act as localized data acquisition centers, termed wireless sensor units (WSUs), that can serve in any role in the active control architecture. In addition to a wireless transceiver, each node is equipped with an on-board microcontroller, a transducer interface (i.e., analog-to-digital converter), and an actuation interface (i.e., pulse width modulator or digital-to-analog-converter). While these nodes have been successfully demonstrated in global control architectures^{4–6}, these studies have also highlighted the challenges of the sensing nodes, such as communication delays due to information bottleneck and computational delays due to the limited computational capacity of the on-board microcontroller. In particular, researchers have found that as they attempt to embed more complex control algorithms onto the microcontroller, the control frequency quickly degrades to values that are borderline effective^{6–9}.

To address latencies due to computational inundation, it is proposed to use the *Martlet*, a high-speed data acquisition node, to serve as both the sensing node and the controller node. Previous research has indicated that this node is a viable option, as it was able to effectively mitigate the effects of seismic base isolation on a partial-scale, single-story structure¹⁰. In this study, the results from that study are extended in complexity and are applied to a partial-scale, four-story structure subject to seismic base isolation.

*peckens@hope.edu; phone 1 616 395-7021

Sensors and Smart Structures Technologies for Civil, Mechanical, and Aerospace Systems 2022, edited by Daniele Zonta, Branko Glisic, Zhongqing Su, Proc. of SPIE Vol. 12046, 1204602 · © 2022 SPIE · 0277-786X · doi: 10.1117/12.2612570

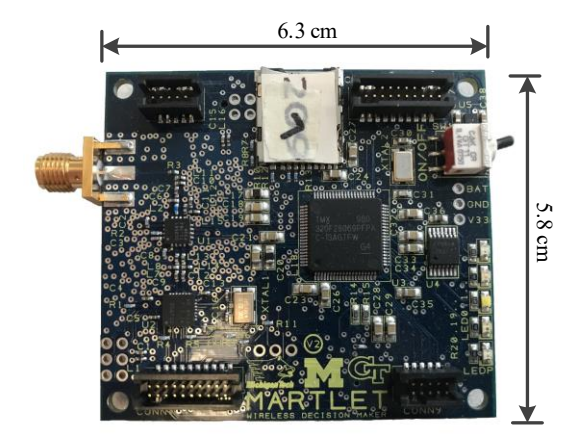


Figure 1. Data acquisition and computing node, *Martlet*.

2. CONTROL ARCHITECTURE

In this study, a traditional control architecture is executed using a high-speed data acquisition and computing node, the *Martlet*¹¹ (Fig. 1). The *Martlet*, developed at the University of Michigan in collaboration with Georgia Institute of Technology and Michigan Technological University, is chosen due to its fast processing capabilities, which greatly reduces computational and communication delays within the system. The *Martlet* was designed with versatility in mind and can easily adapt to different applications through the addition of peripheral boards. In this way, the *Martlet* serves in two distinct roles in the control architecture: the sensor node and the controller node.

In this control architecture, feedback control is executed using the full-state linear quadratic regulator (LQR) optimal control theory. The LQR solution determines an optimal control force, u, through minimizing the performance index, J,

$$J = \int_0^\infty (\mathbf{z}^T \mathbf{Q} \mathbf{z} + \mathbf{u}^T \mathbf{R} \mathbf{u}) dt$$
 (1)

where Q and R are symmetric positive, semi-definite weighting matrices and z is a vector of the system states. This optimization is dependent on the response of the structure, which is assumed to be linear-time invariant, and can, therefore, be modeled through traditional state space equations,

$$\dot{\mathbf{z}} = A\mathbf{z} + B\mathbf{u} \tag{2}$$

$$y = Cz + Du \tag{3}$$

where $\mathbf{z} \in \mathbb{R}^m$ is the state vector, $\mathbf{y} \in \mathbb{R}^q$ is the output vector, $\mathbf{u} \in \mathbb{R}^p$ is the input or control vector, $\mathbf{A} \in \mathbb{R}^{m \times m}$ is the system matrix, $\mathbf{B} \in \mathbb{R}^{m \times p}$ is the input matrix, $\mathbf{C} \in \mathbb{R}^{q \times m}$ is the output matrix, and $\mathbf{D} \in \mathbb{R}^{q \times p}$ is the feed-through matrix given that m is the number of states of the system, q is the number of outputs, and p is the number of inputs. The constant feedback gain vector, \mathbf{K} , is obtained through solving the Ricatti equation during the optimization of equation 1, and this leads to the simplistic control law $\mathbf{u} = \mathbf{K}\mathbf{z}$, where \mathbf{K}_i corresponds to the control gain associated with the i^{th} state of the system.

In order to execute this control law, all states in the system are required. Therefore, based on the state space equations, the control algorithm requires both displacement and velocity measurements. For control purposes, velocity can be approximated from displacement using a Kalman filter but this has been shown to impede the overall control sampling frequency^{8,9}. Instead, a differentiating circuit (Fig. 2b) is integrated into a data acquisition peripheral board (Fig. 2a) which converts the displacement signal directly into a velocity signal. This eliminates computations at the controller node during each execution of a control step. This peripheral board is mounted directly to a *Martlet* sensing node, which then transmits both displacement and velocity to the controller node.

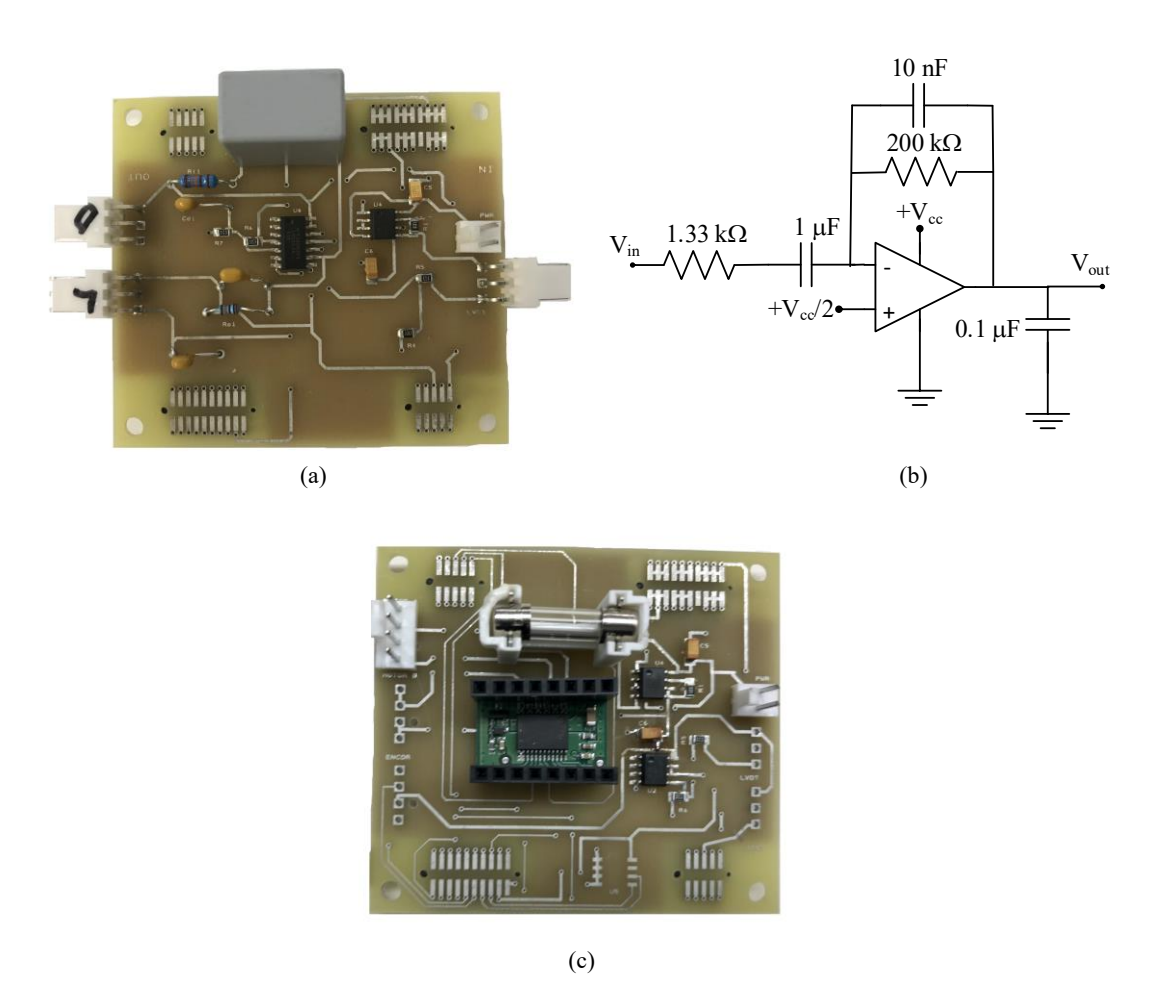


Figure 2. Martlet sensing and differentiating peripheral (a), circuit schematic of differentiating circuit (b), and motor controller peripheral (c). Note on the circuit schematic, V_{cc} is the power supply, V_{in} is the displacement measure, and V_{out} is the resulting velocity. All peripheral boards have dimensions: 6.3cm x 5.8cm.

The *Martlet* also serves as the controller node in the control architecture. The controller node receives information (i.e., displacement and velocity) from the sensing node(s) and calculates the control force, using the control law u = Kz, that is necessary to mitigate the structure's response to some external load. The *Martlet* passes the resulting control force to a mounted motor controller peripheral board (Fig. 2c). The motor controller peripheral board is equipped with the Pololu TB6612FNG Dual Motor driver, which converts commands from the *Martlet* to voltage signals that drive the actuator.

3. EXPERIMENTAL VALIDATION

3.1 Experimental Test Bed

In this study, the control algorithm is experimentally validated on a small-scale, four-story shear structure (Fig. 3). Each floor of the shear structure is comprised of two 10.8 cm x 30.5 cm x 2.54 cm aluminum plates that are connected to the floor below by four T6061 aluminum columns of size 61 cm x 3.8 cm x 0.016 cm. The top floor also includes four additional plates. The structure is attached to a vibration exciter (APS Dynamics Electro-seis) that is able to induce seismic base excitation. An active mass damper (AMD) is placed on floors two and four, which serve as the actuator that mitigates the displacement of the structure resulting from the ground motion. The AMD is an aluminum cart that is manufactured by *Quanser* and is capable of high precision control through the use of its on-board high-quality DC motor and a quadrature encoder. The structure is outfitted with four magnetostrictive linear-position transducers (MTS sensors,

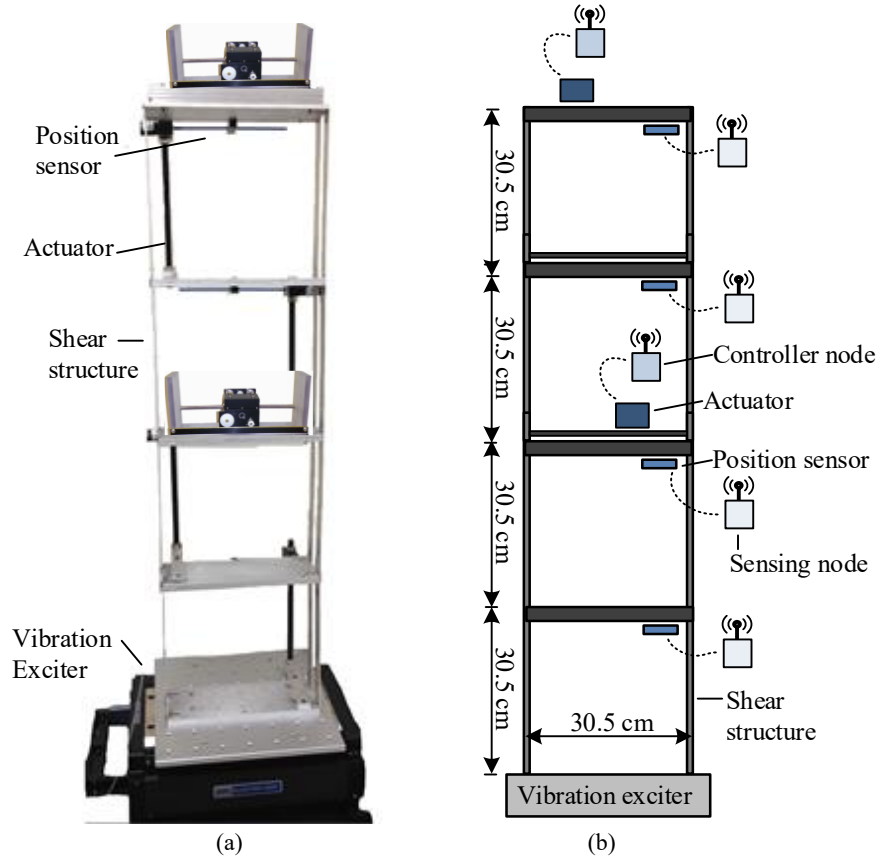


Figure 3. Four-story shear structure (a) and schematic (b).

C-series core sensor) that are connected to the sensor peripheral board and used to measure the structure's displacement. The structure's modal frequencies are 1.53, 3.41, 5.18, and 6.75 Hz, which are found experimentally through the frequency response function using an input sine sweep as the ground motion. The damping of the structure was estimated based on Rayleigh damping that is both mass-proportional and stiffness-proportional, using a 3% damping ratio¹².

3.2 Quantification of Control Effectiveness

The effectiveness of the LQR control law is quantified using four cost functions, adapted from Ohtori et al¹³. Two of these cost functions quantify the minimization of inter-story displacement, which correlates to the damage of nonstructural elements, and the minimization of acceleration, which correlates to occupational comfort. These cost functions are

$$J_{1} = \frac{\max(|\boldsymbol{d}(t)_{controlled}|)}{\max(|\boldsymbol{d}(t)_{(uncontrolled}|)}$$
(4)

where d is a time history vector for each floor in the four-story structure, and

$$J_2 = \frac{\|d(t)_{controlled}\|}{\|d(t)_{uncontrolled}\|}$$
 (5)

where $\|\cdot\|$ denotes the l_2 -norm function. The controlled parameter in these two equations is the scenario when the control law is executed and the uncontrolled parameter is the scenario when no control is executed and the structure response is only due to the seismic event. For quantification of acceleration, a, the cost functions are

$$J_3 = \frac{\max(|a(t)_{controlled}|)}{\max(|a(t)_{uncontrolled}|)}$$
(6)

and

$$J_4 = \frac{\|\boldsymbol{a}(t)_{controlled}\|}{\|\boldsymbol{a}(t)_{uncontrolled}\|}$$
(7)

Because there are four floors in the structure, each cost function is a vector with 4 elements.

3.3 Preliminary Experimental Results

The four-story structure is excited using the 1940 El Centro earthquake record (Fig. 4) and controlled via the LQR method. The resulting cost functions are shown in Table 1 and the uncontrolled versus controlled displacements are shown in Figure 5. In general, this method is able to reduce the maximum displacement (J_1) and the averaged displacement (J_2) for almost all floors. However, the reduction is not as significant as seen in simulation. Additionally, when applying this control technique to a single story, a more significant reduction in the maximum displacement and average displacement occurred, with resulting cost functions of 0.28 and 0.25, respectively¹⁰. The parameters of the control algorithm will continue to be explored in order to improve the response of the four-story structure.

As compared to the displacement metrics, the acceleration metrics (e.g., J_3 and J_4) where not reduced and in most cases the acceleration is increased. The actuators, in this case, have fairly erratic behavior and the motor of the AMD produces significant jitter into the system. It is hypothesized that a on a full-scale system that employs full-scale actuators, the acceleration metrics would be much improved.

4. CONCLUSIONS

Civil infrastructure with integrated feedback control systems is not a new area of research but technology limitations have created several bottlenecks in communication and computational capabilities that prevents its widespread adoption.

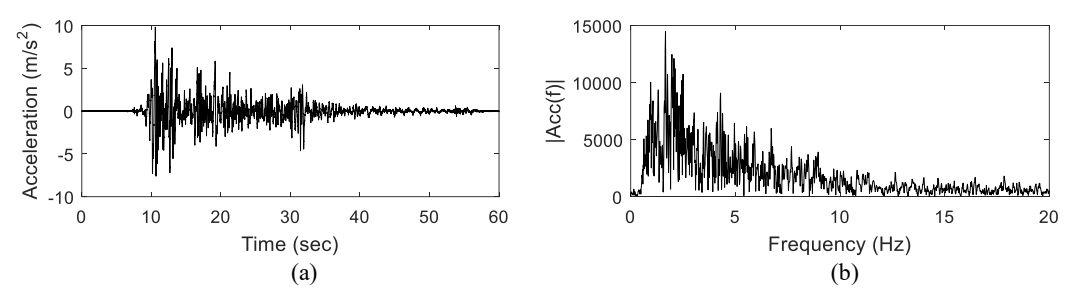


Figure 4. 1940 El Centro (Southeast) Earthquake in the time (a) and frequency (b) domains.

Table 1. Cost functions for four-story structure subject to El Centro earthquake.

Floor Cost Function	1	2	3	4
J_1	1.01	0.943	0.820	0.753
J_2	0.883	0.908	0.788	0.744
J_3	1.22	2.92	1.49	1.57
J_4	0.819	1.42	1.07	1.04

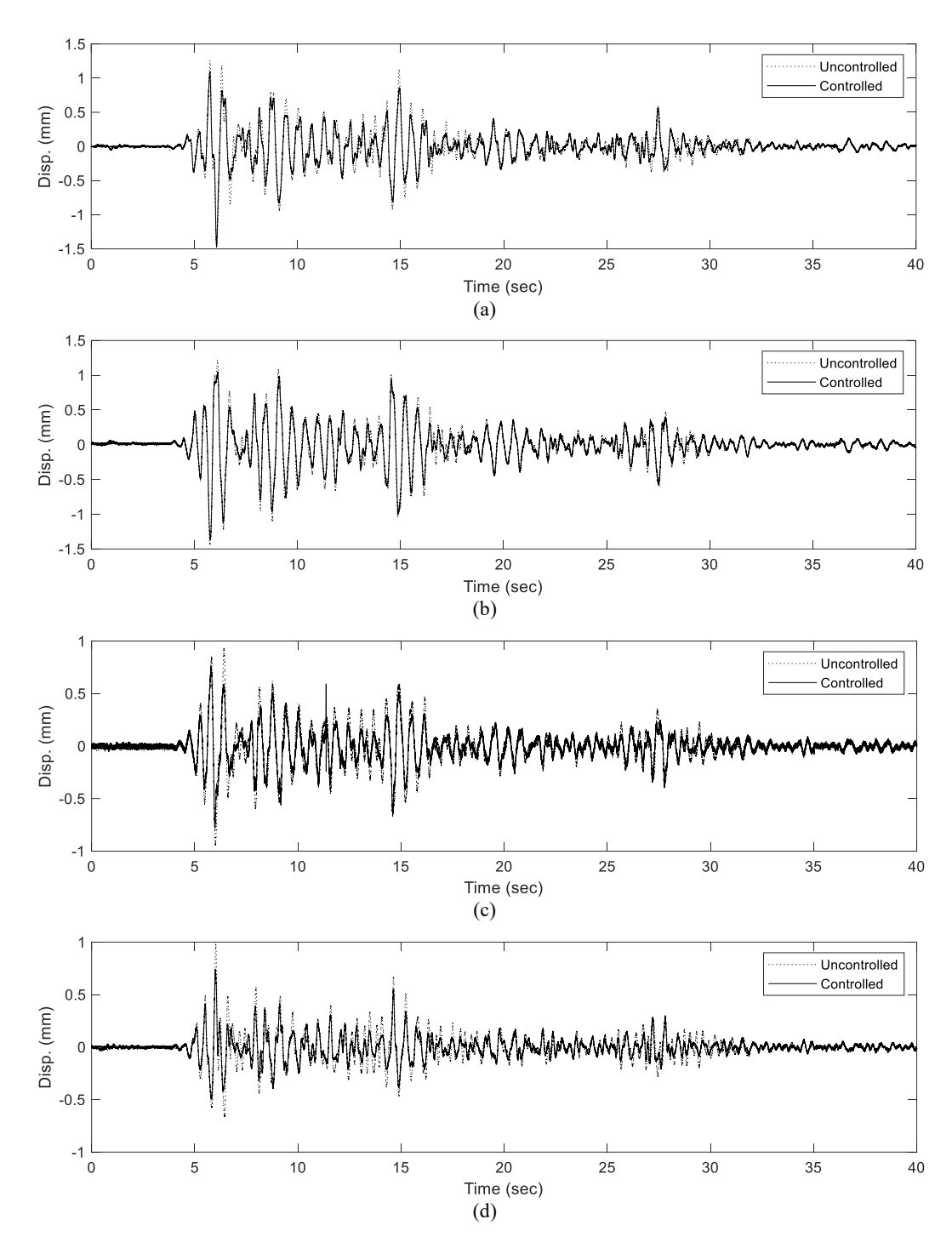


Figure 5. Measured first (a), second (b), third (c), and fourth (d) floor voltages when subject to the El Centro earthquake using the LQR algorithm.

In this study, a high-speed data acquisition computing node is used as both the sensing and controller node to address many of these challenges. By using a differentiating circuit at the sensing node and an optimal control algorithm, the controller node is able to rapidly make control decisions. The effectiveness of this method is applied to a four-story shear structure. This method is able to reduce displacement but not by a substantial amount. Acceleration is not

reduced, in part due to the effects of the motor of the AMD. Future work will include refining the control law in order to improve the effectiveness of control.

5. ACKNOWLEDGMENTS

The authors would like to gratefully acknowledge the generous support offered by the National Science Foundation through Grant Number CMMI-166265. The authors would also like to acknowledge the Hope College undergraduate engineering students who contributed to this project: Anne O'Donnell, Christian Forester, and Rebekah Ludema.

REFERENCES

- [1] Saaed, T. E., Nikolakopoulos, G., Jonasson, J.-E. and Hedlund, H., "A state-of-the-art review of structural control systems," Journal of Vibration and Control **21**(5), 919–937 (2015).
- [2] Housner G. W., Bergman L. A., Caughey T. K., Chassiakos A. G., Claus R. O., Masri S. F., Skelton R. E., Soong T. T., Spencer B. F., and Yao J. T. P., "Structural Control: Past, Present, and Future," Journal of Engineering Mechanics **123**(9), 897–971 (1997).
- [3] Spencer, B. F. and Nagarajaiah, S., "State of the Art of Structural Control," Journal of Structural Engineering 129(7), 845–856 (2003).
- [4] Wang, Y., Swartz, A., Lynch, J. P., Law, K. H., Lu, K.-C. and Loh, C.-H., "Wireless feedback structural control with embedded computing," Health Monitoring and Smart Nondestructive Evaluation of Structural and Biological Systems V 6177, 61770C, International Society for Optics and Photonics (2006).
- [5] Lynch, J. P., Wang, Y., Swartz, R. A., Lu, K. C. and Loh, C. H., "Implementation of a closed-loop structural control system using wireless sensor networks," Structural Control and Health Monitoring **15**(4), 518–539 (2008).
- [6] Swartz R. A. and Lynch J. P., "Strategic Network Utilization in a Wireless Structural Control System for Seismically Excited Structures," Journal of Structural Engineering **135**(5), 597–608 (2009).
- [7] Verdoljak, R. D. and Linderman, L. E., "Sparse feedback structures for control of civil systems," Structural Control and Health Monitoring **23**(11), 1334–1349 (2016).
- [8] Wang, Y., Lynch, J. P. and Law, K. H., "Decentralized $\mathcal{H}\infty$ controller design for large-scale civil structures," Earthquake Engineering & Structural Dynamics **38**(3), 377–401 (2009).
- [9] Spencer, B. F., Jo, H., Mechitov, K. A., Li, J., Sim, S.-H., Kim, R. E., Cho, S., Linderman, L. E., Moinzadeh, P., Giles, R. K. and Agha, G., "Recent advances in wireless smart sensors for multi-scale monitoring and control of civil infrastructure," J Civil Struct Health Monit 6(1), 17–41 (2016).
- [10] Peckens, C. A., Bleitz, E. and O'Donnell, A., "Experimental validation of a proposed bio-inspired control algorithm for civil infrastructure," Active and Passive Smart Structures and Integrated Systems XV, J.-H. Han, S. Shahab, and G. Wang, Eds., 49, SPIE, Online Only, United States (2021).
- [11] Kane, M., Zhu, D., Hirose, M., Dong, X., Winter, B., Häckell, M., Lynch, J. P., Wang, Y. and Swartz, A., "Development of an extensible dual-core wireless sensing node for cyber-physical systems," presented at SPIE Smart Structures and Materials + Nondestructive Evaluation and Health Monitoring, 10 April 2014, San Diego, California, USA, 90611U.
- [12] Chopra, A. K., [Dynamics of structures: theory and applications to earthquake engineering, Fifth edition], Pearson, Hoboken, NJ (2017).
- [13] Ohtori Y., Christenson R. E., Spencer B. F., and Dyke S. J., "Benchmark control problems for seismically excited nonlinear buildings," 4, Journal of Engineering Mechanics **130**(4), 366–385 (2004).